# Post-Print of an Accepted Manuscript on the Laboratory of Turbulent Flows Website

Complete citation:

Rowin, W. A., Asha, A. B., Narain, R., & Ghaemi, S. (2021). A novel approach for drag reduction using polymer coating. *Ocean Engineering*, *240*, 109895. doi: 10.1016/j.oceaneng.2021.109895

The final publication is available at https://doi.org/10.1016/j.oceaneng.2021.109895



The Accepted Manuscript begins on the next page.

# A novel approach for drag reduction using polymer coating

Wagih Abu Rowin[§], Anika Benozir Asha[†], Ravin Narain[†], and Sina Ghaemi[*§]

[§] Department of Mechanical Engineering, University of Alberta, Edmonton, Alberta T6G 2G6, Canada
[†] Department of Chemical and Materials Engineering, University of Alberta, Edmonton, Alberta T6G 2G6, Canada

**Corresponding Author** *E-mail: ghaemi@ualberta.ca

## Abstract

Polymer drag reduction (DR) remains challenging for marine applications due to the difficulties in introducing the polymer drag-reducer into external flows. We developed a novel coating that bonds drag-reducing polymers to metallic surfaces. The coating consists of a polydopamine (PDA) layer that can attach to any substrate. A layer of anionic polyacrylamide (APAM), which is a drag reducing agent, is then grafted on the PDA-coated surface. Owing to the covalent bond, the long chains of APAM polymer slowly dissolve from the PDA-coated surface into water. The drag of surfaces with 0.1 to 0.8 mg $cm^{-2}$ of deposited APAM at three Reynolds numbers, *Re*, of $8\times10^3$, $11\times10^3$, and $16\times10^3$ were investigated in a turbulent channel flow. The maximum amount and duration of DR was achieved for an optimum APAM deposition of 0.4 mg $cm^{-2}$ at *Re* of $16\times10^3$. A large DR of 19% occurred in the first 10 min of the tests, and then gradually reduced to zero within an hour. We also observed that increasing *Re* resulted in a greater initial DR that spanned over a shorter duration, potentially due to a faster dissolving rate of the polymer coating.

## Keywords

Drag reduction, polymer coating, wall-bounded turbulent flows

## 1. Introduction

Reducing the drag associated with turbulent flows has always been an active research area due to its widespread industrial applications. Among the various turbulent drag reduction methods used for liquid flows, the most successful and robust one is the addition of a small amount of a polymer with high molecular weight into the fluid. Toms, (1948) first established this phenomenon, and subsequently its drag-reducing mechanism was investigated by numerous experiments (Ptasinski et al., 2001; White and Mungal, 2008). Polymer drag-reduction typically requires less than 100 weight parts per million (wppm) of the polymer to result in up to 70% drag reduction (Escudier et al., 2009; Ptasinski et al., 2001; Virk et al., 1967). As a result, industry applies polymer drag reduction for reducing pumping costs in various applications including petroleum pipelines, sewage networks, and firefighting systems.

In most laboratory-scale experiments and industrial applications, the drag-reducing polymer mixes with the whole fluid to achieve a homogeneous solution. This method is feasible for internal flows where a finite volume of fluid is present, e.g. for pipe flows. In contrast, for external flows, such as the flow over ships and submarines, it is not feasible to introduce a homogeneous polymer solution as freshwater continuously enters the boundary layer. As an alternative, a concentrated solution of the drag-reducing polymer is injected from the surface into the thin turbulent layer that surrounds the surface. The injected polymer gradually mixes and disperses in the surrounding flow. Since the resulting polymer solution is heterogeneous and its concentration decreases with increasing distance from the injection port, the subsequent drag reduction also varies along the surface (Berman, 1986; Hoyer and Gyr, 1996; Tiederman et al., 1985; Wei and Willmarth, 1992; Willmarth et al., 1987). Therefore, to maintain a constant drag reduction, the polymer should be injected uniformly along the surface, or at least from several locations.

The injection of polymer solution is typically carried out through several surface penetrations into the turbulent boundary layer (Semenov, 1991). For marine applications, such a modification to the vessel hull is not desirable and it remains impractical as the injection orifices reduce the structural integrity of the hull. As a result, it is of interest to introduce the polymer solution into the flow using a method that is not destructive toward the vessel hull. In a novel technique, Motozawa et al., (2010) dispersed polyethylene

oxide (PEO), which is a drag-reducing polymer, into conventional antifouling (AF) paint. To test the coating, they applied it to the inner cylinder of a Taylor-Couette device. They measured the torque using a load cell and compared the drag with a baseline non-coated surface. Their results demonstrated that the PEO dissolved into water and generated an initial drag reduction (DR) of up to 20%. The DR gradually diminished, and after 30 hours, the drag was higher than the non-coated surface. The latter observation was associated with the large roughness of the residual AF paint. It is also important to note that due to the small volume of the Taylor-Couette device (1 liter), a homogeneous polymer solution formed that was also subject to shear-induced degradation. More recently, Yang et al., (2014) also investigated a drag-reducing coating that combined a self-polishing AF paint and PEO. Due to a hydrolysis reaction, the AF coating becomes soluble and gradually erodes, releasing the PEO into the surrounding flow. To reduce the coating roughness, they sieved out the largest PEO particles. The performance of the coating was investigated in several facilities including a Taylor-Couette device, a turbulent channel flow, and two towing facilities. Yang et al., (2014) observed more than 10% DR with respect to the baseline AF paint, while a smaller DR (~2-3%) was observed with respect to a non-coated smooth surface.

The previous investigations show that when the drag-reducing polymer is mixed with an AF paint a rough surface is generated, which can contribute to drag increase. In addition, when the drag-reducing polymer is depleted, the remaining rough AF paint may result in drag increase with respect to a smooth surface (Motozawa et al., 2010; Yang et al., 2014). To address this issue, we have developed a novel technique to apply a polymer coating without using an AF paint. The developed coating consists of dual layers of polydopamine (PDA) and a commercial anionic polyacrylamide (APAM). The technique is inspired by mussel adhesive proteins that enable robust adhesion to a variety of substrates under water. Surface modification with dopamine and other catecholamine derivatives has recently created a universal surface modification platform (Lee et al., 2007). Alkali-induced autoxidation of dopamine into PDA coatings was the most interesting single step surface functionalization method to graft a wide range of polymers subsequently (Liu et al., 2016; Ryu et al., 2018). Because of the high reactivity of a PDA coating towards the nucleophiles, it plays the role of an intermediate linker to immobilize other chemical

components onto the surface and impart the desired property (Chang et al., 2016). In the subsequent sections, we describe the coating procedure, characterize it, and evaluate its drag-reducing performance. For the latter task, we used a turbulent channel flow and measured the pressure drop of the flow.

## 2. Materials and methods

In this section, we first explain the preparation of the polymer coating. Then we briefly describe the flow facility and the measurements used for evaluating the DR performance of the coating.

### 2.1. Formulation and manufacturing of the polymer coating

The polymer coating consists of two layers of polydopamine (PDA) and anionic polyacrylamide (APAM) as shown in Fig. 1. The APAM used has a molecular weight ranging from 12 to 15 Mg/mol and an intrinsic viscosity of 24.29 deciliters per gram, supplied by SNF oil and gas. The PDA layer works as an adhesion layer for the APAM solution. Dopamine hydrochloride (DA), containing both amino and phenolic hydroxyl functional groups, was dissolved into a Tri(hydroxymethyl) amino methane (Tris)-HCl (50 mM, pH 8.5) buffer solution with a concentration of 0.5 mg/mL. pH-induced oxidation of DA changes the solution color to dark brown. Lee et al., (2007) reported that under oxidative conditions dopamine can be self-polymerized to form a single-step thin coating on a wide range of substrates, mimicking the adhesion of Mytilus edulis foot protein. Under oxidative conditions, the hydroxyl groups show deprotonation and become dopamine-quinone. Later via intramolecular cyclization this dopamine-quinone subsequently turns into leukodopaminechrome, which subsequently forms 5,6 dihydroxyindole or 5,6 indolequinone through further oxidation and rearrangement (Bernsmann et al., 2011; Jiang et al., 2011). Inter-molecular crosslinking of 5,6 dihydroxyindole or 5,6 indolequinone through branching reactions finally leads to a melanin-like polymer polydopamine (Bernsmann et al., 2011) (see Fig. 1). Thus, a firmly adherent dopamine into PDA layer can be formed on the surface of a substrate that is immersed in the dopamine solution for a certain time. PDA coating thickness depends on the concentration of dopamine in the solution, deposition time, pH, and supplied oxygen in the solution. The PDA-coated surface layers contain amino groups and phenolic groups, which can react with a variety of molecules via Schiff-base and Michael

addition chemistries to facilely immobilize thiol or amine containing molecules (Zeng et al., 2018). At this point, PDA can be tightly attached to any material by covalent or noncovalent interactions (such as π-π interactions, charge transfer interactions). Thus, using this dopamine chemistry, we had subsequently grafted APAM via a possible Schiff-base or Michael-type addition reaction between oxidized catechols of the PDA-coated surface and the nucleophilic amines of APAM (Yang et al., 2016).

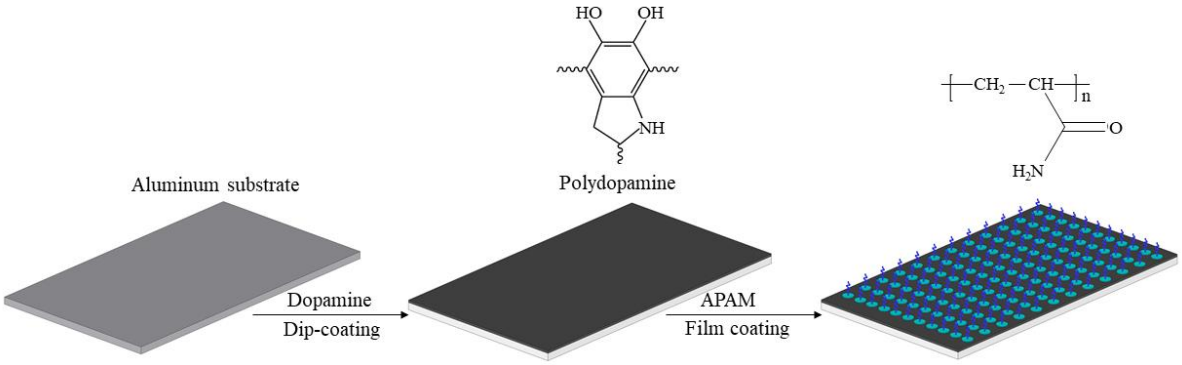


Fig. 1. Scheme of the polymer coating layers starting with the base aluminum substrate on the left side to the APAM film coating on the right side of the Fig..

Aluminum substrates with dimensions of 236×36 $mm^2$ were first ultrasonically cleaned with acetone, ethanol, and deionized water respectively for 30 min each. To achieve a homogeneous thin primary PDA film on the substrates, the cleaned substrates were immersed into a freshly prepared DA solution and shaken at 200 rpm with a mechanical shaker at 25 °C for 12 hours. The coated substrates were washed with deionized water several times and then dried. Due to the great adhesion of PDA with a wide range of polymers, one-step PDA coating has been thoroughly explored as a surface modifier. Prior to the grafting of APAM, the freshly-coated PDA surface was sintered at 70 °C in an oven for 15 mins to get a homogenous surface coverage of the primary coating of PDA (Gibson et al., 2019). Homogenous APAM solutions at different concentrations were prepared by dissolving APAM into a 50:50 mixture of deionized water and ethanol. We prepared six different concentration: 500, 1000, 1500, 2000, 3000 and 4000 weight parts per million (wppm) of APAM polymer solution. The dissolving process was done via magnetic stirring to avoid any mechanical degradation as suggested by Abu Rowin et al., (2018). Using film coatings, a wet layer of homogeneous APAM solution with a thickness of 2.0 mm was deposited on the sintered PDA. After the

film coating process, the coated substrate was dried in an oven and formed a thin PDA/APAM layer. The variation of wppm in the wet-film solution allows us to vary the amount of deposited APAM, *D*, as shown in Table 1.

Table 1. The amount of deposited polymer for different APAM concentrations.

| wppm | $D$ (mg cm$^{-2}$) |
|---|---|
| 500 | 0.1 |
| 1000 | 0.2 |
| 1500 | 0.3 |
| 2000 | 0.4 |
| 3000 | 0.6 |
| 4000 | 0.8 |

The coating topography and thickness were investigated using a Zeiss Sigma 300/VP- FESEM (Carl Zeiss Microscopy Ltd.). A field emission scanning electron microscopy (FESEM) image of a small 10×10 mm$^2$ substrate of a silicon wafer was taken as a reference and shown in Fig. 2(*a*). The FESEM image of the silicon wafer coated with a PDA layer in Fig. 2(*b*) shows a scatter of small roughness features spread over the surface, which are mainly the aggregates of PDA deposited on the surface. The average diameter of these roughness features has a wide range varying from 0.01 to 2 μm. Most of the PDA roughness features were covered when the APAM layer with 0.8 mg/cm$^2$ of polymer was applied, as is shown in Fig. 2(*c*). As can be seen, the PDA/APAM coating does not generate large-scale roughness features that can contribute to an increase in local turbulent drag. The thickness of the PDA/APAM coating was evaluated from a side view FESEM image (e.g., Fig. 2(*d*)) of a silicon wafer coated with a similar coating protocol to what was described in the previous section. After the drying process, the thickness of the combined PDA and APAM layers was approximately 70 μm. The root-mean-square of coating roughness, estimated from the side view FESEM images, was approximately 5.9±0.4 μm. The change of the polymer deposition density did not alter the coating roughness. At the three *Re* of the current study, the coatings are considered

hydrodynamically smooth since the roughness elements submerge in the viscous sublayer (Wu and Patterson, 1989). For the three Reynolds numbers applied here, the estimated linear viscous sublayer varies from 33 to 59 μm which is an order of magnitude larger than the surface roughness. As it was discussed, the pressure drop measurements is carried out 52*H* downstream of the coated plate. Therefore, the surface topology and roughness of the coating does not have any effect on the measured drag reduction.

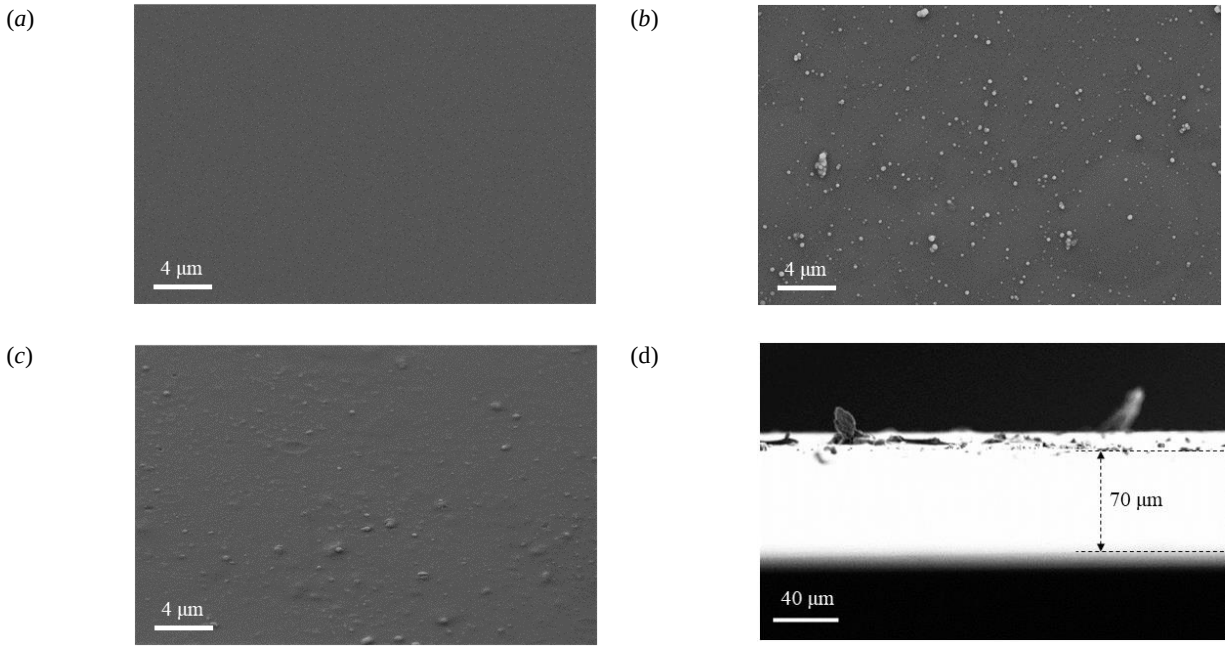


Fig. 2. FESEM images with a top-down view of the (*a*) silicon wafer, (*b*) silicon wafer coated with PDA, and (*c*) silicon wafer coated with PDA and APAM. (*d*) Side view of the PDA/APAM coating after drying in the oven.

## 2.2. Flow facility

The experiments were conducted in a closed-loop turbulent channel flow facility. A schematic diagram of the experiment appears in Fig. 3. The rectangular test section of the channel had a height, *H*, of 6 mm and a width, *W*, of 40 mm. The relatively large aspect ratio of $W/H = 6.7$ ensures a two-dimensional flow in the center of the channel (Dean, 1978; Vinuesa et al., 2014). The total length of the rectangular test section was 200*H* (1.2 m). A replaceable test plate with dimensions of 240×40 $mm^2$ in the streamwise and spanwise directions was installed 42*H* (250 mm) downstream of the channel entrance. A groove with

dimensions of 236×36 mm$^2$ was machined on the test-plate to hold the aluminum substrates flush to the inner surface of the channel. The coated plates were placed close to the entrance to allow the released polymer to mix with the incoming flow, and form a fully developed flow farther downstream, where the pressure drop is measured. A bare aluminum substrate was used as the baseline smooth surface. A centrifugal pump controlled using a variable frequency driver, circulated tap water in the loop. The total volume of water was 50 liters.

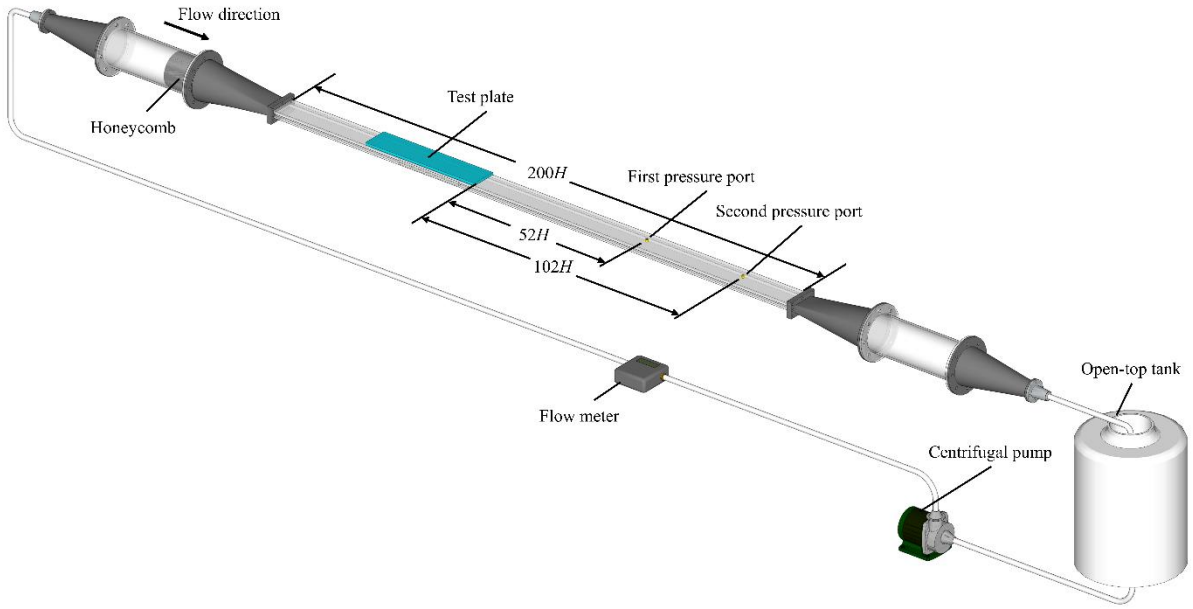


Fig. 3. Schematic diagram of the experimental setup showing the pressure ports and the test plate.

To measure the turbulent drag, we incorporated measurements of pressure drop downstream of the test plate. The two pressure ports were at 130*H* (800 mm) and 180*H* (1100 mm) downstream of the channel entrance. In wall-bounded experiments with polymer injection, there is an initial region where the injected polymer mixes with the incoming flow and drag-reduction significantly varies with streamwise distance. According to the measurement of Tiederman et al., (1985), this region with large variation of drag reduction is limited to a maximum distance of 30*H* downstream of the polymer injection slot. Beyond the streamwise location, the variation in drag reduction and the pressure drop are negligible. In the current investigation, the distance between the downstream edge of the coated surface and the first pressure port is 52*H*, which is

sufficient to measure the drag-reduction. The second pressure port is also 102$H$ downstream of the coated surface. A differential-pressure transducer (P15, Validyne Engineering Corp., Northridge, CA) was connected to a sine wave demodulator (CD15, Validyne Engineering Corp., Northridge, CA) to measure the pressure difference between the two pressure ports. The percentage of DR downstream of the coated surfaces was calculated following

$$\mathrm{DR} = \frac{\Delta P_0 - \Delta P}{\Delta P_0}, \quad (1)$$

where $\Delta P_0$ and $\Delta P$ are the pressure drops over the baseline and the coated surface, respectively. The average velocity across the cross-section, $U$, was set to 1.2, 1.6, and 2.3 m $s^{-1}$, equivalent to Reynolds numbers of $8\times10^3$, $11\times10^3$, and $16\times10^3$. The Reynolds number, $Re$, is defined as $U\,H/v$. Here, $v$ is the kinematic viscosity of the water. All three $Re$ correspond to the turbulent regime. To remove any trapped air, the water was circulated in the facility for 15 min. Then the coated surfaces were installed on the test-plate, and water was circulated for an additional minute before recording the pressure data.

In the experiments, the measurements of pressure drop indicate the effect of the locally dissolved polymer, not the polymer solution that has circulated back into the channel. This is mainly due to the small amount of dissolved polymer in the bulk fluid and high mechanical degradation of the pump. If the maximum amount of deposited polymer (~70 mg based on 0.8 mg $cm^{-2}$) is dissolved in the loop, the final concentration would be 1.4 wppm, which is small to result in a significant DR. In addition, we used a small centrifugal pump at high rotational speeds to ensure that the polymer solution degrades after circulating through the pump (Den Toonder, 1995).

## 3. Results

In this section, we first characterize the surface before and after the DR tests using a Fourier transform infrared (FTIR) spectrophotometer. Then we evaluate the drag measurements for a non-coated surface and discuss the drag measurements for the coated surfaces. The error bars in this section indicate the measurement range (minimum to maximum) estimated from at least two independent experiments for each case.

### 3.1. Surface characterization.

To confirm the polymer grafted to the surface, the coating was characterized by FTIR using an Agilent Technologies Cary 600 Series FTIR spectrometer (ATR mode) between 600 and 3900 $cm^{-1}$. The ATR-FTIR analysis displayed in Fig. 4(*a*, *b*, and *c*) are for the surface of a pristine aluminum substrate with the PDA coating only, a PDA-coated aluminum surface with a freshly-grafted APAM coating (PDA/APAM), and a PDA/APAM-coated aluminum surface after the drag reduction test, respectively. In the latter case, the surface was exposed to water flow for a long time. As shown in Fig. 4(*a*) and Fig. 4(*b*), broad absorbance appears between 3610 and 3720 $cm^{-1}$, ascribed to the N – H/O – H stretching vibration of the PDA coating. The absorption peak at 1409 $cm^{-1}$ represents the phenolic C – O – H bending vibration. The presence of this characteristic absorbance peak confirmed the presence of a thin PDA layer on the surface (Shah et al., 2019). Based on the previous research of Wang et al., (2017) the absorbance peak at 1257 $cm^{-1}$ was assigned to the N – H scissoring vibrations, while the peak at 1510 $cm^{-1}$ was attributed to the C – O stretching from phenolic moieties. Compared to the PDA coating, the new appearance of an absorbance peak at 1664 $cm^{-1}$ in the PDA/APAM spectrum in Fig. 4(*b*) corresponds to C = O stretching in amide groups of polyacrylamide which confirms the successful grafting of APAM to the PDA coated surface (Yang et al., 2010). The absorption peaks at 2890 and 2973 $cm^{-1}$ represent C – H stretching of $CH_2$. The new absorbance peaks at 1648 and 3439 $cm^{-1}$ in the spectrum of the PDA/APAM after drag reduction, in Fig. 4(*c*), were attributed to hydration which proves the successful interaction of the APAM with water in the flow channel (Feng et al., 2017). The presence of broad peaks at 3000 and 3600 $cm^{-1}$ in Fig. 4(*c*) confirms that PDA coating can remain intact after a DR test and creates an opportunity to reuse it to graft APAM again.

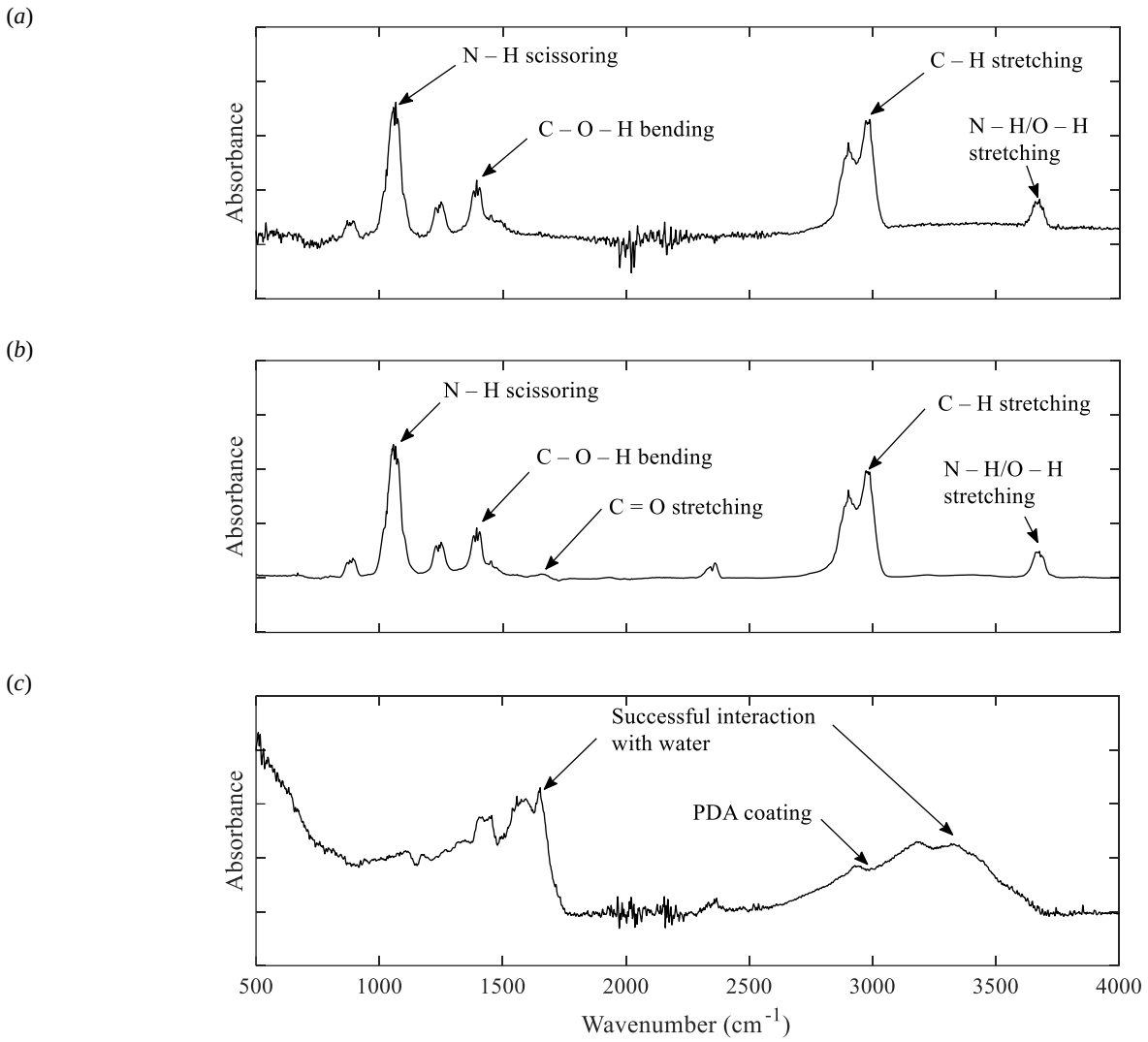


Fig. 4. FTIR measurements of the (*a*) PDA coating, (*b*) PDA/APAM coating, and (*c*) PDA/APAM coating after the DR test.

214

215 The elemental contents on the coated substrate were tested using an energy-dispersive X-ray
216 spectroscopy (EDX), performed using Bruker XFlash. The EDX analysis in Table 2 shows that after
217 grafting APAM on the PDA-coated surface, the nitrogen (N) and oxygen (O) content increased significantly
218 compared to that of the PDA-coated-only surface. The increase of these characteristic contents from APAM
219 also proves the successful grafting of APAM on the PDA surface.

Table 2. Surface elemental composition of the coated surfaces using EDX.

| Sample Name | C | O | N | Si |
|---|---|---|---|---|
| Control (Si wafer) | 37.85 | - | - | 62.15 |
| PDA | 73.65 | 21.68 | 4.66 | - |
| PDA/APAM | 50.53 | 37.95 | 11.52 | - |

### 3.2. Drag of the non-coated surface.

To evaluate the measurement system and to obtain the baseline drag for comparison with the coated surfaces, pressure drop measurements were carried out downstream of the non-coated surface. The measurements are compared with Dean's correlation for turbulent flow expressed as $f = 0.073(Re)^{-0.25}$. Here $f$ is the fanning friction factor. As shown in Fig. 5, the friction factors at the three tested $Re$ of $8\times10^3$, $11\times10^3$, and $16\times10^3$ are comparable to Dean's correlation. The maximum discrepancy between the current measurement and Dean's correlation is about 5% and is mainly associated with the smaller aspect ratio of the channel ($W/H$ = 6.7). The small discrepancy indicates the validity of the current measurements and confirms that a fully developed turbulent flow was present at the measurement location. The repeatability of the measurement, shown by error bars, varies by no more than 7%.

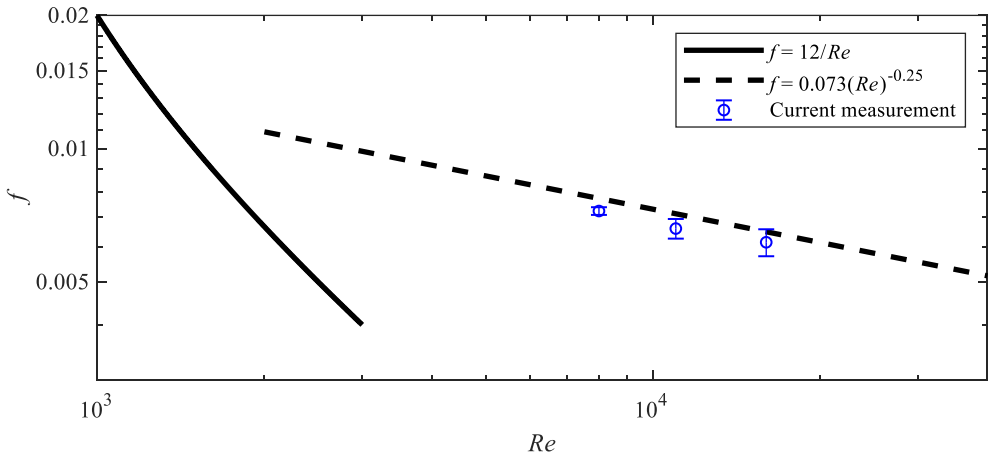


Fig. 5. Friction factor against Reynolds number for the non-coated surface. The Poiseuille equation for the laminar flow ($f$ =12/$Re$) and the Dean's correlation ($f = 0.073Re^{-0.25}$) are also shown.

### 3.3. Drag of the polymer-coated surfaces.

The effect of varying the amount of deposited polymer is shown in Fig. 6. In this figure, DR is shown as a function of time, $T$, during which the coated surfaces was exposed to flow at $Re$ of $16\times10^3$. For a polymer deposition of 0.1 mg cm$^{-2}$, the DR remains negligible, potentially due to the small amount of released polymer. For 0.2 mg cm$^{-2}$, the DR starts at 5% and quickly reduces to zero after 10 min. For higher deposition densities of 0.3 and 0.4 mg cm$^{-2}$, DR remains constant at about 15-20% for the first 20 min of the experiments. The DR gradually reduces and after about 50 min approaches zero. In contrast, a different trend is observed for higher deposition densities of 0.6 and 0.8 mg cm$^{-2}$. At 0.6 mg cm$^{-2}$, DR starts at about 18%, but immediately reduces with increasing time, and reaches zero after 45 min. For the maximum deposition density of 0.8 mg cm$^{-2}$, DR also starts at about 15% and diminishes rapidly within 10 min. The measurements show that the deposition rate of 0.4 mg cm$^{-2}$ results in the maximum DR percentage and duration. At the end of the tests, the APAM coating was completely dissolved in water, while the PDA layer was still available for re-grafting a new layer of APAM if necessary.

Three observations are made from Fig. 6. First, the variation of DR with the amount of deposited polymer indicates that the deposited amount affects the release rate of the polymer into the water. The polymer release rate affects the local polymer concentration and therefore the DR. Second, an optimum amount of deposited polymer can result in a polymer release rate that maximizes DR amount and duration. If a larger amount of polymer is deposited in the coating, DR and its duration decrease. It is hypothesized that for larger amounts of deposited polymer ($D$ = 0.6 and 0.8 mg/cm$^2$), the adhesion of the APAM chains to the PDA layer is weaker. Therefore, the *loose* APAM polymers that are not bonded to the PDA layer, quickly release into water and deplete the polymer supply. This results in the larger initial DR followed by a fast decrease in DR observed for $D$ = 0.6 and 0.8 mg/cm$^2$ cases. Third, the decrease in DR with time indicates that the release rate of the polymer coating also varies in time. The trends show that as the polymer coating erodes and dissolves into the flow, the release rate decreases. It is conjectured that the top APAM layers release quickly, while the bottom APAM layers that are closer to the PDA layer release slower. In general, the deposited amount of APAM controls both the DR percentage and its duration.

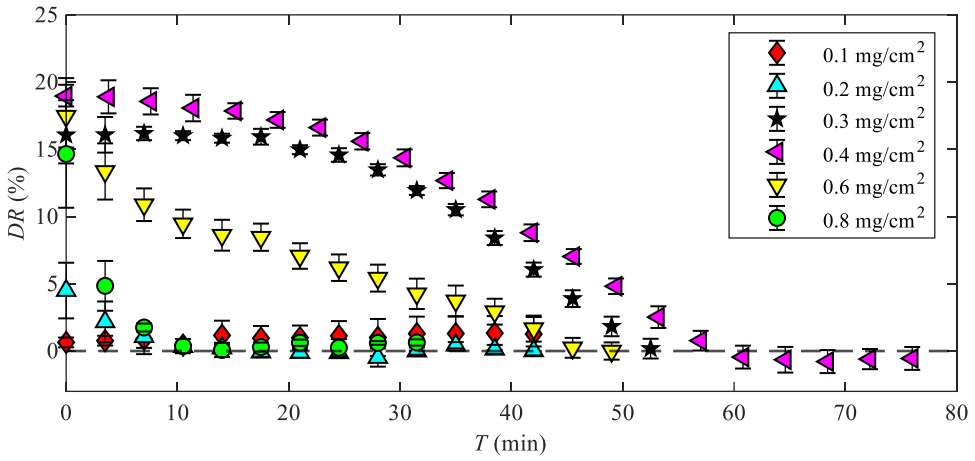


Fig. 6. Effect of APAM deposition on DR at $Re = 16\times10^3$.

To demonstrate the effect of the deposited APAM amount on the initial DR, the DR averaged over the first 10 min, $DR_0$, is shown in Fig. 7 for various values of D. As can be seen, there is a clear trend of increasing $DR_0$ with increasing deposition reaching up to ~19% at 0.4 mg $cm^{-2}$. After this point, higher deposition does not increase $DR_0$, and it reduces to ~5% at 0.8 mg $cm^{-2}$. As we discussed above, this trend is potentially associated with a quick depletion of the APAM layer due to the release of the loose polymers that are present in the thicker layers. Another potential cause of this trend can be the saturation phenomenon reported by Lumley, (1973). Winkel et al., (2009) reported that an excessive polymer concentration increases the drag owing to greater solution viscosity. For example, Warholic et al., (1999) observed 69% DR for an injected polymer concentration of 500 wppm, while a smaller DR of 52% was observed for 1000 wppm. In the current experiment, the excess polymer concentration may not be a factor since the overall DR is smaller than 20%, suggesting that the local viscosity has not reached the saturation limit. In an experimental investigation using a similar polymer, Shaban et al. (2018) measured DR of 25, 43, 51, and 57% for homogeneous polymer solutions with concentrations of 10, 20, 90, and 150 ppm, respectively. Therefore, for the smaller DR of the current experiment, the local polymer concentration is expected to be smaller than 10 ppm.

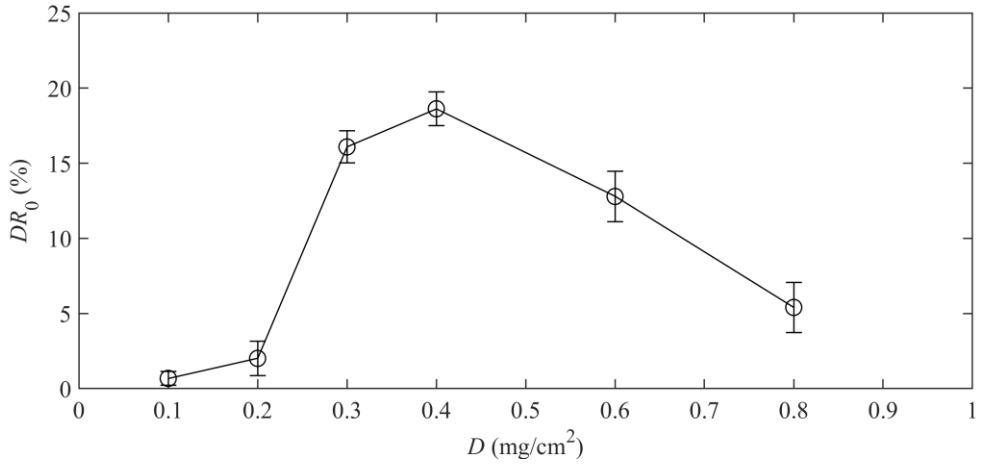


Fig. 7. Drag reduction averaged over the first 10 min.

The variation of *Re* is expected to affect the release and dissolution rates of the polymer layer by changing the shear stress applied to the polymer coating. To investigate the effect of *Re*, the coatings were tested at $Re = 8\times10^3$, $11\times10^3$ and $16\times10^3$ for an initial APAM deposition of 0.6 mg cm$^{-2}$. It is worth noting here that the polymer chain scission (polymer degradation) due to the greater shear rate of the high *Re* flows can decrease the DR (Feng et al., 2017). Based on the analysis of Vanapalli et al., (2005), at the wall-shear-rate of the largest *Re* of $16\times10^3$, the molar mass of the polymers reduces to approximately 8 Mg/mol. At the two smaller *Re*, the wall-shear-rate does not reduce the molecular mass. As seen in Fig. 8, for all the three *Re*, the DR gradually decreases in time. For $Re = 8\times10^3$, the DR started at 13% and reduces to zero after 35 min. Based on visual inspection of the substrate, we observed that a residual layer of APAM remained attached to the substrate at $T = 35$ min. Further exposure to the flow at $Re = 8\times10^3$ resulted in a slow loss of the APAM layer without any considerable DR. Therefore, the shear of the flow was not adequate to efficiently release the APAM coating into the flow. At $Re = 8\times10^3$, visual inspection of the surface showed that after 100 min the entire APAM layer was removed from the surface. However, the DR was negligible beyond the initial 35 min, potentially due to the small polymer release rate.

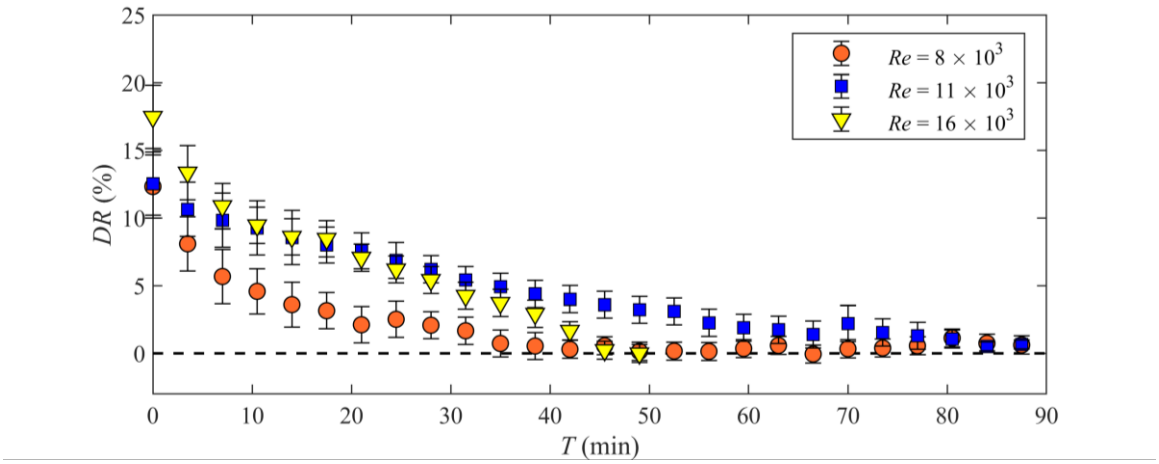


Fig. 8. The effect of *Re* on the DR over time for a surface coated with 0.6 mg cm$^{-2}$ of APAM.

The initial DR for $Re = 11\times10^3$ and $Re = 8\times10^3$ at $T = 0$ are similar and about 12%. In contrast, at $Re = 11\times10^3$, DR persists for a longer time and extends up to approximately 80 min. It is conjectured that the DR is larger for $Re = 11\times10^3$ relative to $Re = 8\times10^3$ due to the higher polymer release rate; the higher flow shear increases the release rate of the APAM coating. Another possibility that may explain the increase in DR with increasing *Re* is reduction of local viscosity due to two mechanisms: (a) the local viscosity at the larger *Re* is smaller since the released polymer mixes with more fluid, (b) the higher shear-rate results in a smaller local viscosity due to the shear thinning behavior of polymeric solutions. However, as it was discussed, the local viscosity of the fluid is expected to be small due to the low DR. The maximum initial DR is obtained at $Re = 16\times10^3$. However, after 8 min of testing, the DR at $Re = 16\times10^3$ approaches that of $Re = 11\times10^3$ and remains comparable until 25 min. Visual inspection of the substrate showed that, after 50 min, the APAM layer was completely removed from the coated substrate, which is consistent with the observed zero DR. The results indicate that the maximum DR percentage and duration are obtained when the flow releases APAM at an optimum rate. For the current experimental condition, $Re = 16\times10^3$ results in a larger initial DR while $Re = 11\times10^3$ extends the DR over a longer period for the surface with $D = 0.6$ mg/cm$^2$.

## 4. Conclusion

We developed and tested a novel polymer coating strategy utilizing dual layers of polydopamine (PDA) and anionic polyacrylamide (APAM). The layer of PDA acted as a primary coating on the surface, allowing to subsequently graft a layer of APAM over it. The PDA layer was obtained by immersing the cleaned substrate in a container filled with dopamine hydrochloride solution for 12 hours. A layer of APAM solution was then applied over a freshly prepared and sintered PDA-coated surface using a film coating technique. The coated surface was dried in oven before any characterization or testing was carried out. To confirm the presence of the dual polymer layers on the substrate, the coated surfaces were first characterized with ATR-FTIR. The results proved the presence of both the PDA and APAM coatings, revealing their characteristic absorbance peaks. Field emission scanning electron microscopy images were then taken to analyze the coating topography and thickness. The images showed that the coating did not introduce any large roughness features relative to the base surface. The root-mean-square roughness of the coating was approximately 5.9±0.4 μm for different amounts of deposited APAM. The thickness of the two-layer coating after drying was ~70 μm for maximum APAM deposition of 0.8 mg $cm^{-2}$.

The drag of a turbulent channel flow downstream of the coated surfaces was monitored using pressure drop measurements carried out at streamwise distances of 52*H* and 102*H* downstream of the coated surface. We varied the amount of deposited APAM from 0.1 to 0.8 mg $cm^{-2}$, and operated the channel at Reynolds numbers, *Re*, of $8\times10^3$, $11\times10^3$, and $16\times10^3$. The results showed that 0.4 mg $cm^{-2}$ of APAM resulted in the highest initial drag reduction (DR) of 19%, which gradually reduced to zero over an hour. For smaller APAM depositions of 0.1 and 0.2 mg $cm^{-2}$, the initial DR was less than 5% and diminished within 10 min. An initial DR of approximately 15% was observed for larger deposition amounts of 0.6 and 0.8 mg $cm^{-2}$, but the DR diminished faster relative to the 0.4 mg $cm^{-2}$ case. The shorter duration of DR for larger polymer depositions is mainly associated with a weaker adhesion between APAM and PDA layers, which resulted in a fast deposition of the APAM layer. Therefore, the results show that optimum polymer release-rate can be obtained by controlling the amount of deposited polymer. The polymer release rate also varied with *Re*. At the lowest *Re* of $8\times10^3$, a sufficient amount of APAM was not released into the flow and the resulting DR was small. At the highest *Re* of $16\times10^3$, a large initial DR was observed, but it quickly diminished as

the deposited polymer depleted. A slightly smaller initial DR was observed for a *Re* of $11\times10^3$, however, the DR lasted longer. In general, the results show that the release rate of the polymer, and therefore the DR, is a function of the amount of deposited polymer and the flow *Re*. The deposited polymer amount should be adjusted to obtain the optimum release rate that results in maximum DR.

The developed polymer coating technique showed a considerable DR, offering a cost-effective alternative to the injection of water-soluble polymers. In the current investigation, the DR lasted for about an hour; therefore, the application of this coating is currently limited to systems in which a large DR is sought for a short time-period. Further optimization of the coating is needed to increase its longevity and extend its application. Moreover, due to the dynamic nature of the PDA, some catechol or hydroxyl group will always be available for the re-grafting of APAM or any other polymer onto the PDA-coated surface, which makes this approach a quick and easy way to re-engineer the surface if required.

## 5. Acknowledgments

The authors are grateful for the financial support of the Natural Sciences and Engineering Research Council of Canada (Strategic Partnership Project STPGP 494070 - 16).

## 6. References

Abu Rowin, W., Sean Sanders, R., Ghaemi, S., 2018. A Recipe for Optimum Mixing of Polymer Drag Reducers. J. Fluids Eng. 140, 1–10. https://doi.org/10.1115/1.4040109

Berman, N.S., 1986. Velocity fluctuations in non-homogeneous drag reduction. Chem. Eng. Commun. 42, 37–51. https://doi.org/10.1080/00986448608911735

Bernsmann, F., Ball, V., Addiego, F., Ponche, A., Michel, M., Gracio, J.J.D.A., Toniazzo, V., Ruch, D., 2011. Dopamine-melanin film deposition depends on the used oxidant and buffer solution. Langmuir 27, 2819–2825. https://doi.org/10.1021/la104981s

Chang, C.C., Kolewe, K.W., Li, Y., Kosif, I., Freeman, B.D., Carter, K.R., Schiffman, J.D., Emrick, T., 2016. Underwater Superoleophobic Surfaces Prepared from Polymer Zwitterion/Dopamine Composite Coatings. Adv. Mater. Interfaces 3. https://doi.org/10.1002/admi.201500521

Dean, R.B., 1978. Reynolds Number Dependence of Skin Friction and Other Bulk Flow Variables in Two-Dimensional Rectangular Duct Flow. J. Fluids Eng. 100, 215–223. https://doi.org/10.1115/1.3448633

Den Toonder, J.M.J., 1995. Degradation Effects of Dilute Polymer Solutions on Turbulent Drag Reduction

in Pipe Flows 63–82.

Escudier, M.P., Nickson, A.K., Poole, R.J., 2009. Turbulent flow of viscoelastic shear-thinning liquids through a rectangular duct: Quantification of turbulence anisotropy. J. Nonnewton. Fluid Mech. 160, 2–10. https://doi.org/10.1016/j.jnnfm.2009.01.002

Feng, L., Zheng, H., Gao, B., Zhang, S., Zhao, C., Zhou, Y., Xu, B., 2017. Fabricating an anionic polyacrylamide (APAM) with an anionic block structure for high turbidity water separation and purification. RSC Adv. 7, 28918–28930. https://doi.org/10.1039/C7RA05151D

Gibson, C.T., Ridings, C.R., Blok, A.J., Shearer, C.J., Andersson, G.G., Ellis, A. V., 2019. Morphological changes of sintered polydopamine coatings. Surf. Topogr. Metrol. Prop. 7. https://doi.org/10.1088/2051-672X/ab06eb

Hoyer, K., Gyr, A., 1996. Turbulent velocity field in heterogeneously drag reduced pipe flow. J. Nonnewton. Fluid Mech. 65, 221–240. https://doi.org/10.1016/0377-0257(96)01460-7

Jiang, J., Zhu, Liping, Zhu, Lijing, Zhu, B., Xu, Y., 2011. Surface characteristics of a self-polymerized dopamine coating deposited on hydrophobic polymer films. Langmuir 27, 14180–14187. https://doi.org/10.1021/la202877k

Lee, H., Dellatore, S.M., Miller, W.M., Messersmith, P.B., 2007. Mussel-inspired surface chemistry for multifunctional coatings. Science. 318, 426–430. https://doi.org/10.1126/science.1147241

Liu, M., Zeng, G., Wang, K., Wan, Q., Tao, L., Zhang, X., Wei, Y., 2016. Recent developments in polydopamine: An emerging soft matter for surface modification and biomedical applications. Nanoscale. https://doi.org/10.1039/c5nr09078d

Lumley, J.L., 1973. Drag Reduction in Turbulent Flow by Polymer Additives. J. Polym. Sci. Macromol. Rev. 7, 263–290.

Motozawa, M., Ito, T., Matsumoto, A., Ando, H., Ashida, T., Senda, T., Kawaguchi, Y., 2010. Turbulent Drag Reduction by Polymer Containing Paint: Simultaneous Measurement of Skin Friction and Release Rate 1–9.

Ptasinski, P.K., Nieuwstadt, F.T.M., van den Brule, B.H.A.A., Hulsen, M.A., 2001. Experiments in turbulent pipe flow with polymer additives at maximum drag reduction. Flow, Turbul. Combust. 66, 159–182. https://doi.org/10.1023/A:1017985826227

Ryu, J.H., Messersmith, P.B., Lee, H., 2018. Polydopamine Surface Chemistry: A Decade of Discovery. ACS Appl. Mater. Interfaces. https://doi.org/10.1021/acsami.7b19865

Semenov, B.N., 1991. The pulseless injection of polymeric additives into near-wall flow and perspectives of drag reduction. pp. 293–308. https://doi.org/10.1007/978-94-011-3526-9_15

Shaban, S., Azad, M., Trivedi, J., & Ghaemi, S. (2018). Investigation of near-wall turbulence in relation to polymer rheology. Physics of Fluids, 30(12), 125111.

Shah, A.A., Cho, Y.H., Choi, H. gyu, Nam, S.E., Kim, J.F., Kim, Y., Park, Y.I., Park, H., 2019. Facile integration of halloysite nanotubes with bioadhesive as highly permeable interlayer in forward osmosis membranes. J. Ind. Eng. Chem. 73, 276–285. https://doi.org/10.1016/j.jiec.2019.01.039

Tiederman, W.G., Luchik, T.S., Bogard, D.G., 1985. Wall-layer structure and drag reduction. J. Fluid Mech. 156, 419–437. https://doi.org/10.1017/S0022112085002178

Toms, B.A., 1948. Some observations on the flow of linear polymer solutions through straight tubes at large Reynolds numbers. Proc. 1st Int. Congr. Rheol. 2, 135–141.

Vanapalli, S.A., Islam, M.T., Solomon, M.J., 2005. Scission-induced bounds on maximum polymer drag reduction in turbulent flow 095108. https://doi.org/10.1063/1.2042489

Vinuesa, R., Noorani, A., Lozano-durán, A., Khoury, G.K. El, Schlatter, P., Fischer, P.F., Nagib, H.M., Vinuesa, R., Noorani, A., Lozano-durán, A., Khoury, G.K. El, 2014. Aspect ratio effects in turbulent duct flows studied through direct numerical simulation 5248. https://doi.org/10.1080/14685248.2014.925623

Virk, P.S., Merrill, E.W., Mickley, H.S., Smith, K.A., Mollo-Christensen, E.L., 1967. The Toms phenomenon: Turbulent pipe flow of dilute polymer solutions. J. Fluid Mech. 30, 305–328. https://doi.org/10.1017/S0022112067001442

Wang, K., Dong, Y., Yan, Y., Zhang, S., Li, J., 2017. Mussel-inspired chemistry for preparation of superhydrophobic surfaces on porous substrates. RSC Adv. https://doi.org/10.1039/c7ra04790h

Warholic, M.D., Massah, H., Hanratty, T.J., 1999. Influence of drag-reducing polymers on turbulence: effects of Reynolds number, concentration and mixing. Exp. Fluids 27, 461–472. https://doi.org/10.1007/s003480050371

Wei, T., Willmarth, W.W., 1992. Modifying turbulent structure with drag-reducing polymer additives in turbulent channel flows. J. Fluid Mech. 245, 619. https://doi.org/10.1017/S0022112092000600

White, C.M., Mungal, M.G., 2008. Mechanics and Prediction of Turbulent Drag Reduction with Polymer Additives. Annu. Rev. Fluid Mech. 40, 235–256. https://doi.org/10.1146/annurev.fluid.40.111406.102156

Willmarth, W.W., Wei, T., Lee, C.O., 1987. Laser anemometer measurements of Reynolds stress in a turbulent channel flow with drag reducing polymer additives. Phys. Fluids 30, 933. https://doi.org/10.1063/1.866278

Winkel, E.S., Oweis, G.F., Vanapalli, S.A., Dowling, D.R., Perlin, M., Solomon, M.J., Ceccio, S.L., 2009. High-Reynolds-number turbulent boundary layer friction drag reduction from wall-injected polymer solutions. J. Fluid Mech. 621, 259–288. https://doi.org/10.1017/S0022112008004874

Wu, H., Patterson, G.K., 1989. Laser-Doppler Measurements Of Turbulent-Flow Parameters In A Stirred Mixer. Chem. Eng. Sci. 44, 2207–2221.

Yang, J., Saggiomo, V., Velders, A.H., Stuart, M.A.C., Kamperman, M., 2016. Reaction pathways in catechol/primary amine mixtures: A window on crosslinking chemistry. PLoS One 11. https://doi.org/10.1371/journal.pone.0166490

Yang, W.J., Park, H., Hwan Chun, H., Ceccio, S.L., Perlin, M., Lee, I., 2014. Development and performance at high Reynolds number of a skin-friction reducing marine paint using polymer additives. Ocean Eng. 84, 183–193. https://doi.org/10.1016/j.oceaneng.2014.04.009

Yang, Z., Wang, J., Luo, R., Maitz, M.F., Jing, F., Sun, H., Huang, N., 2010. The covalent immobilization of heparin to pulsed-plasma polymeric allylamine films on 316L stainless steel and the resulting effects on hemocompatibility. Biomaterials. https://doi.org/10.1016/j.biomaterials.2009.11.091

Zeng, Y., Liu, W., Wang, Z., Singamaneni, S., Wang, R., 2018. Multifunctional Surface Modification of Nanodiamonds Based on Dopamine Polymerization. Langmuir 34, 4036–4042. https://doi.org/10.1021/acs.langmuir.8b00509